Khảo sát khả năng hấp phụ malachite green của hệ vi hạt fibroin tơ tằm phối trộn poly(vinylpyrrolidone)

TÓM TẮT

Nghiên cứu chế tạo các hệ vi hạt từ fibroin tơ tằm có phối trộn poly(vinylpyrrolidone) (PVP) ứng dụng xử lí malachite green. Fibroin được chiết từ kén tằm khô đạt hiệu suất 22,91±1,21%. Các hệ vi hạt FNPs và PVP-FNPs được tổng hợp bằng phương pháp đổi dung môi có kích thước lần lượt là 136 nm và 578 nm sẽ được ứng dụng trong việc loại bỏ malachite green (MG) bằng phương pháp hấp phụ. Khả năng hấp phụ malachite green trong nước ảnh hưởng của các yếu tố: nồng độ, khối lượng, thời gian và pH. Kết quả phân tích phổ hồng ngoại biến đổi Fourier (FT-IR) của FNPs và PVP-FNPs chỉ ra các tín hiệu đặc trưng của fibroin tơ tằm, PVP. Quá trình hấp phụ MG tối ưu khi pH 8 trong thời gian 15 phút ở nhiệt độ phòng (25±1℃) với nồng độ MG ban đầu là 80 mg/L đạt hiệu suất là 70,79±1,59% đối với hệ vi hạt FNPs và đạt 74,55±0,86 ở hệ vi hạt 1%-PVP-FNPs. Quá trình hấp phụ của hai hệ vi hạt tuân theo mô hình đẳng nhiệt Freundlich và phương trình động học hấp phụ biểu kiến bậc 2.

Từ khóa*: fibroin, hệ vi hạt, tơ tằm, malachite green, hấp phụ*

Investigation of malachite green adsorption by silk fibroin nanoparticles blended with poly(vinylpyrrolidone)

ABSTRACT

This research aimed to fabricate silk fibroin nanoparticles (FNPs) blended with poly(vinylpyrrolidone) (PVP) for malachite green (MG) dye adsorption. Fibroin extraction from dry silkworm cocoons yielded 22.91±1.21%. The nanoparticles, prepared via solvent-exchange method, had average diameters of 136 nm (FNPs) and 578 nm (1%-PVP-FNPs). Parameters such as dye concentration, adsorbent dosage, adsorption time, and pH were examined for their influence on MG adsorption performance. Fourier-transform infrared (FT-IR) spectroscopy confirmed characteristic peaks of silk fibroin and PVP. Optimal MG adsorption occurred at pH 8, over 15 minutes, at room temperature (25 °C), with an initial MG concentration of 80 mg/L, yielding adsorption efficiencies of 70.79±1.59% for FNPs and 74.55±0.86% for 1%-PVP-FNPs. The adsorption data closely fit the Freundlich isotherm model and pseudo-second-order kinetic equation.

Keywords: *fibroin, nanoparticles, silk, malachite green, adsorption*

1. INTRODUCTION

In recent years, rapid industrial development has negatively impacted the environment, especially concerning water pollution. A major cause of this problem is wastewater discharge from industrial zones. Industries such as paper and pulp production, textiles, cosmetics, and food processing frequently utilize synthetic dyes for product coloration, resulting in substantial releases of hazardous chemicals into the environment. Although textile wastewater contains various pollutants, synthetic dyes are considered the most concerning due to their high usage volumes. Only a small fraction of these dyes adhere to fabrics, while the remainder is discharged directly into the environment. The extensive use of chemicals and dyes in the textile industry is regarded as a principal contributor to water pollution. However, due to their low biodegradability, effectively removing these dyes remains a significant challenge in industrial wastewater treatment. Among commonly used dyes, malachite green (MG) warrants particular attention. MG has been reported as carcinogenic, mutagenic, and teratogenic, posing health risks even at low concentrations.[1] Furthermore, MG can metabolize into leucomalachite green, a residue capable of bioaccumulation and toxicity in organisms.[2] Thus, treating wastewater containing MG before environmental discharge is mandatory to protect public health and water quality.

Currently, various methods have been studied for dye removal, including membrane filtration, electrochemical treatments, photocatalysis, and adsorption. Among these, adsorption is highly valued due to its simple structure, high removal efficiency, and minimal production of hazardous byproducts. Numerous studies have been published on MG removal using adsorption techniques, such as research utilizing Cu/ZIF materials combined with hydrogen peroxide by Pham Tran Bao Nghi et al. (2023),[3] calcium silicate synthesized from waste materials by Amira A. Hashem et al.,[4] kiwi peel-based biosorbents by Yanjun Zhao et al.,[1] and calcined kaolin by Yumeung Wang et al.[5] These studies demonstrated adsorption's feasibility and efficiency in removing MG from wastewater. However, enhancing adsorption efficiency necessitates ongoing research into novel materials or improvements to existing adsorbents. Nanoparticle-based adsorbents are promising candidates due to their advantageous properties such as large surface area, high porosity, substantial surface energy, and functional versatility. Nanoparticles can facilitate electrostatic, hydrophobic, and hydrogen bond interactions with MG molecules, thereby enhancing dye removal efficiency.[6]

Recently, fibroin, a natural protein extracted from silkworm cocoons, has attracted attention in nanoparticle synthesis due to its biodegradability, non-toxicity, and amphiphilic properties, enabling structural transformation into nanoparticles with minimal solvent assistance.[7] Additionally, incorporating polymers like poly(vinylpyrrolidone) (PVP) has been

shown to control nanoparticle size and shape during synthesis, thus broadening potential applications.

However, no previous research in Vietnam has reported combining fibroin and PVP for MG dye removal. Therefore, this work aimed to explore the combined potential of these two materials, laying groundwork for future in-depth research.

2. METHODS

2.1. Materials

Dry silkworm cocoons were purchased directly from local agricultural producers in Nam Dinh province, Vietnam. Chemicals utilized in this research included PVP, $CaCl_2$, Na_2CO_3, $Ca(NO_3)_2$, MG, and ethanol, sourced from Xilong Chemical Co. (China). Double-distilled water was used throughout the experiments.

2.2. Fibroin extraction from silkworm cocoons

The extraction process began with 10 g of silkworm cocoons, which underwent sericin removal using a 0.5% Na_2CO_3 solution at 80 ℃ for 1 hour, followed by thorough washing and drying. Subsequently, the obtained silk fibers were dissolved in a solvent mixture of $CaCl_2$:H_2O:$Ca(NO_3)_2$:EtOH (30:45:5:20, w/w/w/w) at 85-90 ℃ under microwave irradiation (900 W, 2 minutes). The resulting fibroin solution underwent dialysis at room temperature for 3-5 days, then was centrifuged at 10,000 rpm for 30 minutes to eliminate impurities. The final fibroin concentration was determined spectrophotometrically via UV-Vis at a maximum wavelength of 276 nm and stored refrigerated for subsequent experiments.

2.3. Synthesis of PVP-Fibroin nanoparticles

PVP solutions at 0%, 2%, 4%, and 6% were dissolved in 2% (w/v) fibroin solution, maintaining a PVP:Fibroin ratio of 1:1 (v/v), resulting in solutions with final PVP concentrations of 0%, 1%, 2%, and 3%. Exactly 1 mL of each solution was transferred to centrifuge tubes, followed by the gradual addition of 6 mL ethanol (99.5%) as a coagulation agent. Upon ethanol addition, a translucent suspension appeared, and the mixture was shaken for 1 hour to induce β-sheet structure formation in fibroin, resulting in nanoparticle formation. The mixtures were stored overnight at 4 °C, and the particles were collected by centrifugation at 6,000 rpm for 30 minutes, washed with distilled water, and stored refrigerated for further use.

2.4. Malachite Green (MG) adsorption

FNPs or PVP-FNPs particles were dispersed in conical flasks containing 20 mL of MG solution and shaken at 120 rpm at ambient temperature. Adsorption performance was evaluated under varying conditions: MG concentrations (20, 40, 60, 80, 100 mg/L), adsorbent mass ratios (Fibroin or Fibroin/PVP to ethanol: 0.5:3, 1:6, 2:12, 4:24, 6:36, denoted as 0.5, 1, 2, 4, 6), adsorption durations (1, 5, 10, 15, 30, 45, 60, 90, 120 minutes), and solution pH values (2, 4, 6, 8). After each adsorption test, the mixtures were cold-centrifuged, and the remaining MG concentration was measured. Adsorption efficiency (%) was calculated as:

$$\%H = \frac{C_0 - C}{C_0} \times 100$$

where C_0 and C represent initial and residual MG concentrations, respectively (mg/L).

2.5. Physicochemical characterization

The average particle size and polydispersity index (PI) were measured using dynamic light scattering (DLS) with a MicroTrac S3500 analyzer. Fibroin-polymer interactions were evaluated via FT-IR spectra (FT/IR 6300, Jasco, Japan; wavenumber range 400–4000 cm^{-1}) using KBr pellet technique.

Surface charge (pHpzc) determination involved preparing 20 mL of 0.1 M KCl solution adjusted to pH values of 2, 4, 6, 8, 10, and 12 using 0.1 M NaOH or HCl. FNPs or PVP-FNPs were added and shaken at 150 rpm for 24 hours, after which equilibrium pH was recorded. The pHpzc values were identified via graphical methods.

2.6. Adsorption Equilibrium Models

The Langmuir isotherm: :

$$\frac{q_e}{q_m} = \theta = \frac{K_L C_e}{1 + K_L C_e}$$

The Freundlich isotherm:

$$q_e = K_F . C_e^{1/n}$$

where q_e and q_m denote equilibrium and maximum adsorption capacities (mg/g), C_e is the coverage degree, equilibrium concentration (mg/L), and K_L the Langmuir constant, K_F is the Freundlich adsorption constant

The Dubinin-Radushkevich (D-R) model for adsorption nature assessment:

$$\ln q_e = \ln q_m - \beta\varepsilon^2$$

with $\varepsilon = RT\ln(1 + \frac{1}{Ce})$, where β is adsorption energy constant (mol^2/J^2), $E=1/\sqrt{2\beta}$ is

adsorption energy (kJ/mol), indicating adsorption type (physical <8 kJ/mol, chemical 8-16 kJ/mol).

The Temkin isotherm model:

$$q_e = \frac{RT}{b_T}\ln(K_T C_e)$$

where K_T is Temkin constant related to heat adsorption (kJ/mol).

Pseudo-first-order kinetics:

$$\ln(q_e - q_t) = \ln(q_e) - k_1 t$$

Pseudo-second-order kinetics:

$$\frac{t}{q_t} = \frac{1}{k_2 q_e^2} + \frac{t}{q_e}$$

where q_e, q_t are adsorption amounts at equilibrium and time, respectively; k_1, k_2 are respective rate constants. Kinetic parameters were determined by linear regression, evaluating accuracy by correlation coefficient (R^2).

3. RESULTS AND DISCUSSIONS

3.1 Fibroin extraction results

After sericin removal from 10 g of silkworm cocoons using 0.5% Na_2CO_3 solution and drying, 7.55 g of insoluble silk fibers were obtained. From 5 g of these dried fibers, treatment with a salt mixture under microwave irradiation yielded a viscous fibroin-containing solution. This mixture underwent dialysis to eliminate salts and subsequent centrifugation to remove impurities. The resulting fibroin solution was freeze-dried, resulting in 1.145 ± 0.013 g fibroin, corresponding to an extraction yield of 22.91 ± 1.21%.

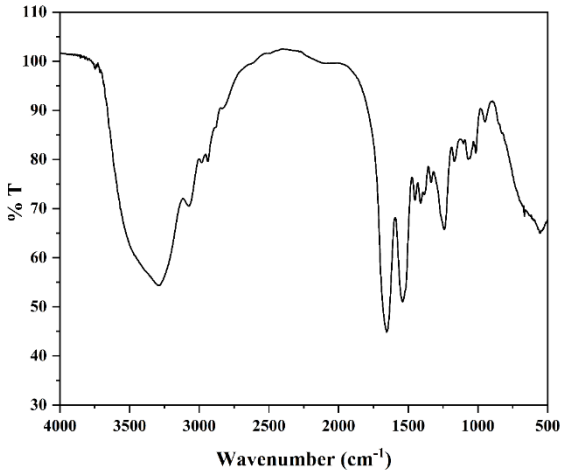

Figure 1. FT-IR spectra of fibroin

FT-IR spectral analysis (**Figure 1**) confirmed fibroin's structure, with characteristic peaks at 1626-1620 cm^{-1} (amide I, C=O stretching), 1525-1515 cm^{-1} (amide II, N-H bending), and 1240-1234 cm^{-1} (amide III, C-N and N-H groups). These peaks indicate β-sheet (silk II) structure, insoluble in water, consistent with findings reported by Pham Duy Toan et al. (2018).[8]

3.2 Particle size and surface charge of nanoparticles

Particle size analysis (**Table 1**) demonstrated successful fabrication of fibroin nanoparticles (FNPs, PVP-FNPs). Particle sizes for blends containing PVP (1%-PVP-FNPs, 2%-PVP-FNPs, 3%-PVP-FNPs) were 578, 623, and 724 nm, respectively, significantly larger than FNPs (136 nm). PVP, containing both strongly hydrophilic pyrrolidone and hydrophobic alkyl groups,[9] likely interacts with fibroin through hydrogen bonds and hydrophobic interactions, creating larger aggregates. Increasing PVP concentration from 1% to 3% proportionally increased particle size due to enhanced PVP-protein interactions and network formation around nanoparticles.

Table 1. Size of PVP-blended fibroin nanoparticles at concentrations of 1, 2, 3%

Samples	Size (nm)
FNPs	136
1%-PVP-FNPs	578
2%-PVP-FNPs	623
3%-PVP-FNPs	724

The pHpzc results (**Figure 2**) showed minimal difference between FNPs (pH_{pzc} 6.8) and 1%-PVP-FNPs (pH_{pzc} 6.9). Thus, these particles are positively charged below their pHpzc and negatively charged above it, predicting effective adsorption of cationic MG at pH > pH_{pzc}.[10]

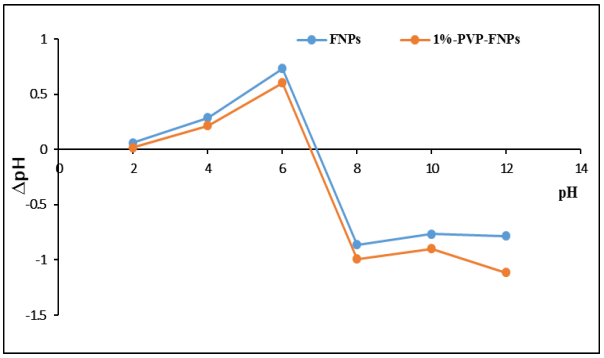

Figure 2. pH_{pzc} graph of FNPs and 1%-PVP-FNPs

3.3 Chemical interactions

Components FT-IR spectra (**Figure 3**) indicated minimal structural differences between 1%-PVP-FNPs and pure FNPs. Characteristic PVP peaks appeared at 1750-1660 cm^{-1} (C=O), 3400-3000 cm^{-1} (N-H stretching), 2970-2820 cm^{-1} (C-H stretching), 1300-1200 cm^{-1} (C-N stretching), and 1450-1420 cm^{-1} (C-H bending).[11] Overlaps with amide bands of fibroin and intensity changes in the 2970-2820 cm^{-1} (C-H) and 3400-3000 cm^{-1} (N-H) bands confirmed PVP's incorporation into the nanoparticles. After adsorption, characteristic peaks of MG appeared at 1160 cm^{-1} (C-N stretching), 1600-1500 cm^{-1} (aromatic C=C), and 800-700 cm^{-1} (C-H bending). The FT-IR spectra thus verified interactions among fibroin, PVP, and MG.

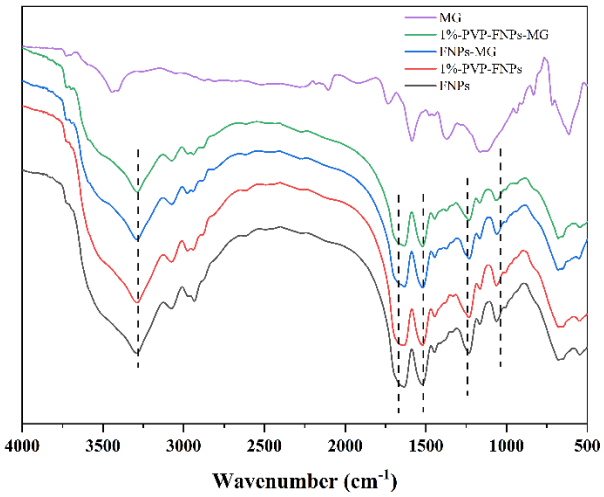

Figure 3. FT-IR spectra of the particles before and after MG adsorption

3.4 Effect of initial MG concentration on adsorption

Increasing initial MG concentration to 80 mg/L yielded maximum adsorption efficiency of 70.57% (FNPs) and 63.14% (1%-PVP-FNPs), which declined to 66.30% and 56.75%, respectively, at 100 mg/L (**Figure 4**). Adsorption capacity significantly increased from 12.09 to 209.31 mg/g (FNPs) and from 6.15 to 96.92 mg/g (1%-PVP-FNPs). Higher initial MG concentrations enhance concentration gradients, promoting rapid MG diffusion initially, but saturation at 80 mg/L suggests that available adsorption sites became fully occupied. Thus, an initial concentration of 80 mg/L was optimal for further tests.

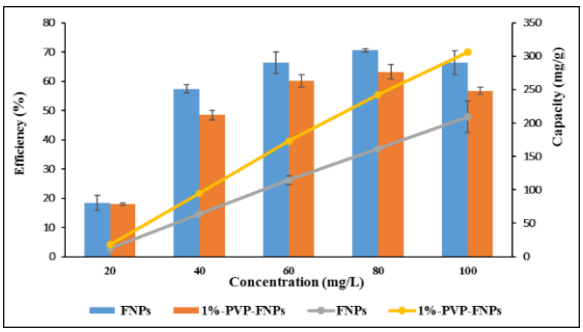

Figure 4. Graph of concentration effect on adsorption efficiency

3.5 Effect of adsorbent amount on adsorption

Increasing nanoparticles amount decreased adsorption capacity due to constant MG availability and increased adsorbent mass. Specifically, FNP adsorption capacity dropped from 179.57 to 29.75 mg/g, and 1%-PVP-FNPs from 115.99 to 17.46 mg/g when dosage increased from 0.5 to 6 g (**Figure 5**).

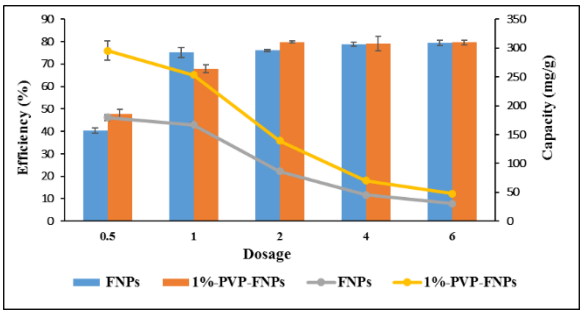

Figure 5. Graph of mass effect on adsorption capacity

3.6 Effect of contact time on adsorption

Adsorption efficiency increased from 66.67% to 77.26% (FNPs) and 69.33% to 74.83% (1%-PVP-FNPs) as contact time increased from 1 to 120 minutes (**Figure 6**). Rapid initial adsorption indicates plentiful available active sites initially, followed by slower adsorption as equilibrium approached around 45 minutes.

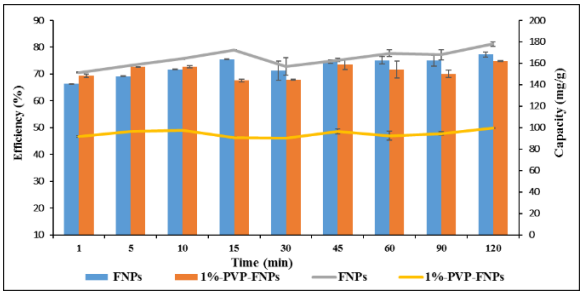

Figure 6. Graph of the effect of time on adsorption capacity

3.7 Effect of pH on adsorption

Increasing solution pH from 2 to 8 significantly improved adsorption efficiency and capacity: from 21.68% to 70.79% (57.34 to 159.15 mg/g) for FNPs and 22.39% to 74.55% (28.32 to 99.43 mg/g) for 1%-PVP-FNPs (**Figure 7**). At lower pH, positively charged sites repel MG cations, whereas higher pH creates negatively charged adsorbent surfaces, enhancing cationic MG adsorption due to electrostatic attraction.

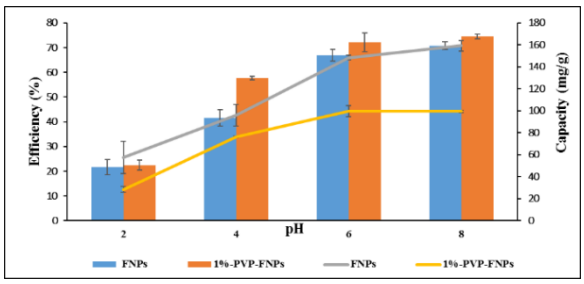

Figure 7. Graph of pH effect on adsorption capacity

3.8 Adsorption equilibrium

Langmuir and Freundlich adsorption isotherms revealed that the Freundlich model (R^2 = 0.814 for FNPs and R^2 = 0.8319 for 1%-PVP-FNPs) described adsorption better, indicating heterogeneous surface adsorption with multilayer formation (**Figure 8**). Temkin constants (0.0062 and 0.0217 kJ/mol, respectively) confirmed physisorption due to low adsorption energy. D-R isotherm energies (E = 0.0483 and 0.1569 kJ/mol) further confirmed physisorption dominated by electrostatic and van der Waals interactions (**Table 2**).

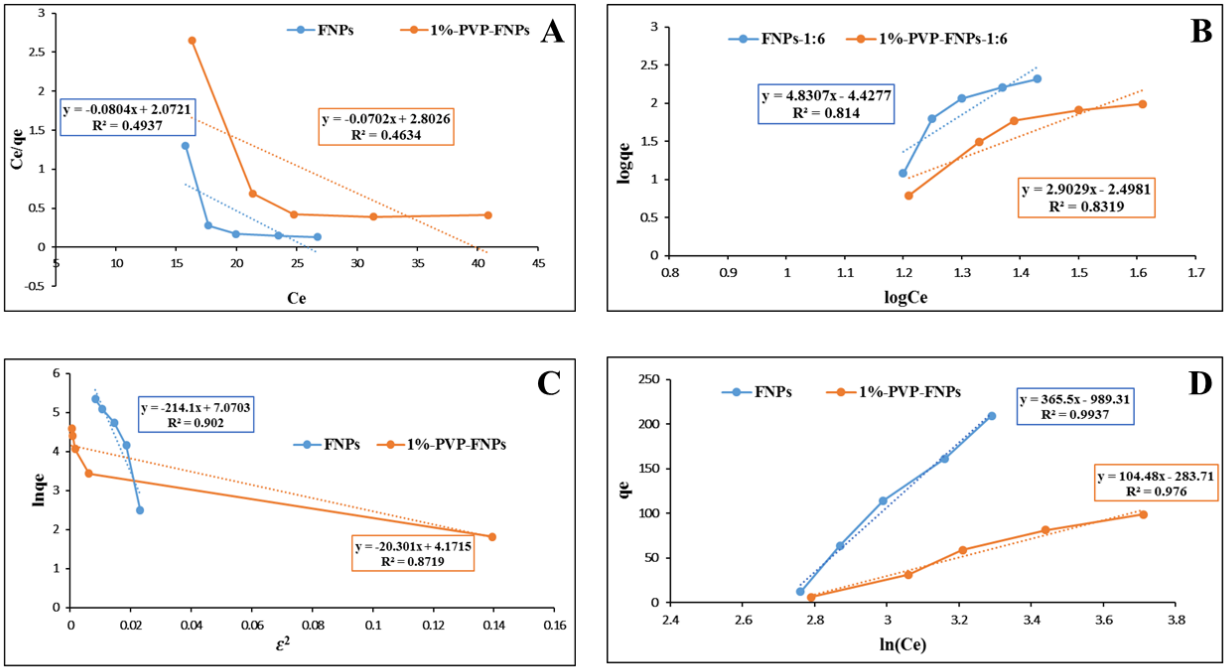

Figure 8. Isothermal models (A) Langmuir, (B) Freundlich, (C) D-R, (D) Temkin

Table 2. Parameters of Temkin and D-R adsorption isotherm models of FNPs and 1%-PVP-FNPs

	FNPs		**1%-PVP-FNPs**	
	Temkin	**D-R**	**Temkin**	**D-R**
$\mathbf{b_T}$	0.0062	-	0.0217	-
$\boldsymbol{\beta}$	-	214.10	-	20.301
E	-	0.0483	-	0.1569
$\mathbf{R^2}$	0.9937	0.9020	0.9760	0.8719
	Langmuir	**Freundlich**	**Langmuir**	**Freundlich**
$\mathbf{q_{max}}$ **(mg/g)**	12.44	-	14.25	-

K_L (L/mg)	0.037	-	0,023	-
K_F	-	0.000037	-	0.0032
n	-	0.21	-	0.34
R^2	0.4937	0.814	0.4634	0.8319

3.9 Adsorption kinetics

Pseudo-first and pseudo-second-order kinetic models indicated superior fitting of the pseudo-second-order equation (high R^2), matching experimental adsorption capacities closely (**Figure 9** and **Table 3**). Smaller slope values suggested fast adsorption kinetics, aligning with high initial adsorption (>60% efficiency in the first minute), validating rapid MG uptake by both nanoparticle systems.

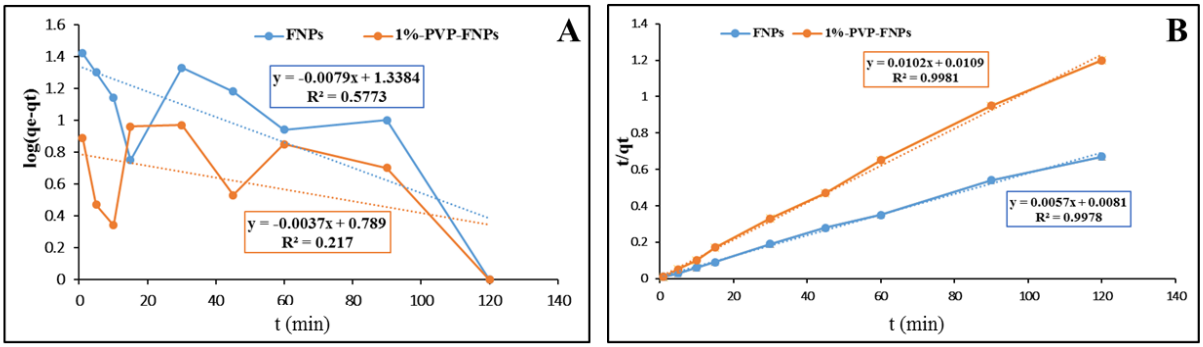

Figure 9. (A) Pseudo-first-order kinetics, (B) Pseudo-second-order kinetics

Table 3. Parameter values of first- and second-order kinetic equations

Pseudo-first-order kinetics	**a**	**b**	**q_e (mg/g)**	**k_1 (1/min)**	**R^2**
FNPs	-0.0079	1.3384	3.81	-0.0079	0.5773
1%-PVP-FNPs	-0.0037	0.7890	2.20	-0.0037	0.217
Pseudo-second-order kinetics	**a**	**b**	**q_e (mg/g)**	**k_2 (g/mg.min)**	**R^2**
FNPs	0.0057	0.0081	175.44	0.0003	0.9978
1%-PVP-FNPs	0.0102	0.0109	98.04	0.0010	0.9981

4. CONCLUSIONS

The study successfully synthesized fibroin nanoparticles blended with PVP for the adsorption of MG. The particle size of fibroin nanoparticles without polymer blending was approximately 136 nm, while the polymer blended system had a size of around 578 nm. The adsorption process occurred rapidly, achieving an adsorption efficiency of over 70% and followed the pseudo-second-order kinetic model.

REFERENCES

1. Y. Zhao, X. Liu, W. Li, S. Pei, Y. Ren, X. Li, C. Qu, C. Wu, J. Liu. Efficient and selective adsorption of cationic dye malachite green by Kiwi-Peel-Based biosorbents, *Molecules*, **2023**, 28, 5310
2. M. Kadhom, N. Albayati, H. Alalwan, M. Al-Furaiji. Removal of dyes by agricultural waste, *Sustainable Chemistry and Pharmacy*, **2020**, 16, 100259
3. P. T. B. Nghi, T. B. Huy, H. N. T. Tân, Đ. H. Giao. Nghiên cứu sử dụng vật liệu Cu/ZIF làm xúc tác xử lý malachite green với sự có mặt của hydrogen peroxide,

Tạp chí Khoa học Đại học cần Thơ, **2023,** 59, 81–89.

4. A. Hashem, S. A. Mahmoud, R. A. Geioushy, O. A. Fouad. Adsorption of malachite green dye over synthesized calcium silicate nanopowders from waste materials, *Materials Science and Engineering: B*, **2023**, 295, 116605
5. Y. Wang, W. Li, H. Ma, W. Guo, and H. Jiang, "Adsorption of malachite green by calcined kaolin as adsorbent: optimization, thermodynamic and kinetics studies," Journal of Physics: Conference Series, **2022**, 2343, 1, 012026
6. C. T. Umeh, A. B. Akinyele, N. H. Okoye, S.S. Emmanuel, K. O. Iwuozor, I. P. Oyekunle, J. O. Ocheje, J. O. Ighalo. Recent approach in the application of nanoadsorbents for malachite green (MG) dye uptake from contaminated water: A critical review," *Environmental Nanotechnology, Monitoring & Management*, **2023**, vol. 20, 100891
7. D. T. Pham, N. Saelim, and W. Tiyaboonchai. Alpha mangostin loaded crosslinked silk fibroin-based nanoparticles for cancer chemotherapy, *Colloids and surfaces. B, Biointerfaces***,** **2019**, 181, 705–713
8. D. T. Pham, N. Saelim, and W. Tiyaboonchai. Crosslinked fibroin nanoparticles using EDC or PEI for drug delivery: physicochemical properties, crystallinity and structure, *Journal of Materials Science*, **2018**, vol. 53, 14087–14103
9. K. M. Koczkur, S. Mourdikoudis, L. Polavarapu, and S. E. Skrabalak. Polyvinylpyrrolidone (PVP) in nanoparticle synthesis, *Dalton Trans***,** **2015**, 44, 41, 17883–17905,
10. Ebtehal A. Al-Maliky, Hatem A. Gzar, Mohammed G. Al-Azawy, Determination of Point of Zero Charge (PZC) of Concrete Particles Adsorbents, *IOP Conference Series: Materials Science and Engineering*, **2021**, 1184 012004
11. A. Safo, M. Werheid, C. Dosche, M. Oezaslan, The role of polyvinylpyrrolidone (PVP) as a capping and structure-directing agent in the formation of Pt nanocubes, *Nanoscale Adv*, **2019**, 1, 3095-3106